Radiation from oscillating dipoles immersed in a solid, and radiation-induced luminescence

Oakley H. Crawford and R. H. Ritchie
Health and Safety Research Division, Oak Ridge National Laboratory, Oak Ridge, Tennessee 37831
(Received 3 August 1987)

We have solved Maxwell's equations for a source, consisting of an oscillating dipole, located in a plane-bounded dielectric half space. Formulas are given for the radiation yield from this source in the region outside the dielectric. The medium is characterized by a local, complex dielectric function $\epsilon(\omega)=\epsilon_1(\omega)+i\epsilon_2(\omega)$. The application of these formulas to the analysis of experimental data on luminescence from solids is discussed, and calculations are presented for aluminum, carbon, silver, copper, and gold.

I. INTRODUCTION

The effect of a nearby dielectric on the radiation from an oscillating dipole has been of considerable interest since the early days of radio. Relevant basic theory was worked out long ago by Sommerfeld,[1] who interpreted a portion of his solution of Maxwell's equations as a wave propagating along the earth's surface. In modern terminology the latter is a variety of surface polariton.[2–4] Renewed interest in this subject has originated from basic studies of light emission from dielectric materials bombarded by electrons[5] and in photon-surface plasmon coupling through surface roughness,[6] especially in connection with surface-enhanced Raman scattering from molecules adsorbed on noble metals.[7]

Photoluminescence, or fluorescence, of metals was discovered by Mooradian,[8] who observed and analyzed the emission of visible light from copper and gold under illumination by visible and ultraviolet light. Mooradian attributed this emission to radiative recombination of electrons and holes generated by optical excitation. As he pointed out, such observations might provide a technique to investigate the band structure of solids, as well as the scattering mechanisms of electrons and holes. This has stimulated considerable interest, recently reviewed in Refs. 9 and 10, in the measurement and interpretation of light emission from metals, under conditions believed to favor this recombination radiation over other luminescence mechanisms such as transition radiation, plasmon emission, and bremsstrahlung.

It is clear that the spectrum, angular distribution, and polarization of light escaping from within a solid may be strongly affected by the optical properties of the medium. However, allowance for the refractive and absorptive properties of the medium seems to have been made in only two recent studies.[11,12] The purpose of the present work is to develop formulas for the effects of the optical properties of a solid on the characteristics of luminescence arising from electronic transitions (including radiative recombination) inside the medium.

We have solved Maxwell's equations for the radiation field outside a semi-infinite medium due to an oscillating dipole immersed in the medium. The latter is supposed to be characterized by a complex, local dielectric function. This solution is necessary for the proper theoretical interpretation of luminescence spectra, particularly when the optical properties of the luminescing medium vary appreciably in the frequency range where luminescence occurs. The formulas presented below should enable one to predict some characteristics of luminescence based on the optical properties alone, and aid in distinguishing such features from others that depend on properties of emitting states. Calculations are presented for aluminum, carbon, silver, copper, and gold, and comparison is made with experiment where possible.

II. THEORY

It is convenient to work with the Hertz vector $\mathbf{\Pi}(\mathbf{r},t)$, which satisfies the wave equation[3]

$$\nabla\times\nabla\times\mathbf{\Pi}-\nabla(\nabla\cdot\mathbf{\Pi})+\frac{\epsilon}{c^2}\frac{\partial^2}{\partial t^2}\mathbf{\Pi}=\frac{4\pi}{\epsilon}\mathbf{P}_e\ , \tag{1}$$

where $\mathbf{P}_e$ is the prescribed polarization, or dipole moment per unit volume of the source, and ϵ is the frequency-dependent complex dielectric function,

$$\epsilon=\epsilon_1+i\epsilon_2\ . \tag{2}$$

The magnetic susceptibility is assumed to be unity. The Gaussian system of units[13] is used, except where otherwise specified.

The electric and magnetic fields are calculable from the Hertz vector, using the following relations:[3]

$$\mathbf{E}=\nabla(\nabla\cdot\mathbf{\Pi})-\frac{\epsilon}{c^2}\frac{\partial^2}{\partial t^2}\mathbf{\Pi}\ , \tag{3}$$

$$\mathbf{H}=\frac{\epsilon}{c}\frac{\partial}{\partial t}(\nabla\times\mathbf{\Pi})\ , \tag{4}$$

using the customary convention that the physical values of fields are given by the real parts of the complex quantities. The above relations are equivalent to Maxwell's equations for nonmagnetic media.

We consider a point dipole of moment $\mathbf{p}(t)$,

$$\mathbf{p}(t)=\mathbf{p}e^{-i\omega t}\ , \tag{5}$$

located in the medium at the point $(0,0,-z_0)$. The

medium is supposed to be bounded by the plane $z=0$, with $\epsilon=1$ in the region $z>0$. The prescribed polarization $\mathbf{P}_e$ is then given by

$$\mathbf{P}_e=\mathbf{p}(t)\delta(x)\delta(y)\delta(z+z_0)\ . \tag{6}$$

We solve first for the Fourier transform $\mathbf{\Pi}_\kappa(z)$, where the transform is defined by the relation,

$$\mathbf{\Pi}(\mathbf{r},t)=\frac{1}{2\pi}\int_{-\infty}^{\infty}d\kappa_x\int_{-\infty}^{\infty}d\kappa_y e^{i(x\kappa_x+y\kappa_y)}\mathbf{\Pi}_\kappa(z)e^{-i\omega t}\ . \tag{7}$$

Equation (1) becomes

$$\left[\frac{d^2}{dz^2}+\frac{\epsilon\omega^2}{c^2}-\kappa^2\right]\mathbf{\Pi}_\kappa^<(z)=-\frac{4\pi}{\epsilon}\mathbf{P}_{e\kappa}(z)\ , \tag{8a}$$

$$\left[\frac{d^2}{dz^2}+\frac{\omega^2}{c^2}-\kappa^2\right]\mathbf{\Pi}_\kappa^>(z)=0\ , \tag{8b}$$

with

$$\mathbf{P}_{e\kappa}(z)=\frac{\mathbf{p}}{2\pi}\delta(z+z_0)\ , \tag{9}$$

where

$$\mathbf{\Pi}=\begin{cases}\mathbf{\Pi}^<, & z\le 0\ ,\\ \mathbf{\Pi}^>, & z>0\ .\end{cases}$$

The method of solution will be described below.

Next, we determine $\mathbf{\Pi}(\mathbf{r},t)$ in the far zone ($r\omega/c\gg1$, $r/z_0\gg1$), using the saddle-point method to perform the inverse Fourier transformation. Then the far-zone fields and the radiated power are found. In general, the power per unit area is given by the time-averaged Poynting vector (Ref. 14), $\bar{\mathbf{S}}=(c/8\pi)\mathbf{E}\times\mathbf{H}^*$. In the far zone, $\mathbf{E}\times\mathbf{H}^*=(\mathbf{E}\cdot\mathbf{E}^*)\hat{\mathbf{r}}$, so the power radiated per unit solid angle $dW/d\Omega$ as observed at point $\mathbf{r}$ in the far zone is given by

$$\frac{dW}{d\Omega}=\frac{c}{8\pi}r^2\mathbf{E}\cdot\mathbf{E}^*\ , \tag{10}$$

where $\mathbf{E}$ is evaluated at $\mathbf{r}$.

In the following, it is convenient to locate the x axis in the plane of observation. The latter is the plane containing the vectors $\mathbf{r}$ and $\hat{\mathbf{z}}$, which are directed toward the observer, and along the outward surface normal, respectively. Then $\mathbf{r}$ is given in terms of its Cartesian (xyz) coordinates by $(r\sin\theta,0,r\cos\theta)$. The polar angle θ is the angle of observation, measured from $\hat{\mathbf{z}}$.

A. Dipole oriented perpendicular to the surface

First we take the vector $\mathbf{p}$ perpendicular to the surface, $\mathbf{p}=p\hat{\mathbf{z}}$. Then an acceptable solution of Eqs. (8) may be written

$$\begin{aligned}\mathbf{\Pi}_\kappa^<&=\mathbf{A}e^{-i\eta z}+\mathbf{\Lambda}e^{i\eta|z+z_0|}\ ,\\ \mathbf{\Pi}_\kappa^>&=\mathbf{A}'e^{i\eta_0 z}\ ,\end{aligned} \tag{11}$$

where

$$\begin{aligned}\eta&=\left[\frac{\epsilon\omega^2}{c^2}-\kappa^2\right]^{1/2}\ ,\\ \eta_0&=\left[\frac{\omega^2}{c^2}-\kappa^2\right]^{1/2}\ ,\end{aligned} \tag{12}$$

and where the coefficients $\mathbf{A}$, $\mathbf{\Lambda}$, and $\mathbf{A}'$ are vectors parallel to $\hat{\mathbf{z}}$, whose magnitudes are functions of κ_x and κ_y. Throughout, the argument of the square root is chosen to lie in the upper half of the complex plane excluding the negative real axis. Since $\mathbf{\Pi}$ is in the z direction, $\mathbf{\Pi}_\kappa=\Pi_\kappa\hat{\mathbf{z}}$, and the transformed expressions for the fields [using Eqs. (3) and (4)] are

$$\mathbf{E}_\kappa=\left[i\kappa_x\frac{\partial\Pi_\kappa}{\partial z},i\kappa_y\frac{\partial\Pi_\kappa}{\partial z},\left[\frac{\partial^2}{\partial z^2}+\frac{\epsilon\omega^2}{c^2}\right]\Pi_\kappa\right]\ , \tag{13}$$

$$\mathbf{H}_\kappa=(\kappa_y,-\kappa_x,0)\frac{\omega\epsilon}{c}\Pi_\kappa\ , \tag{14}$$

so that the standard conditions of continuity of the tangential components of $\mathbf{E}$ and $\mathbf{H}$ at $z=0$ lead to

$$\frac{\partial}{\partial z}\Pi_\kappa^>=\frac{\partial}{\partial z}\Pi_\kappa^<,\quad z=0 \tag{15a}$$

$$\Pi_\kappa^>=\epsilon\Pi_\kappa^<,\quad z=0\ . \tag{15b}$$

Substitution of Eq. (11) for Π_κ in Eqs. (8) and (15) leads to linear equations, which are solved for the coefficients. The result for the Hertz vector outside the medium is

$$\mathbf{\Pi}_\kappa^>=\hat{\mathbf{z}}p\frac{2i}{\eta+\epsilon\eta_0}e^{i(\eta_0 z+\eta z_0)}\ . \tag{16}$$

The inverse Fourier transformation, performed by the saddle-point method, gives the following expression for the Hertz vector in the far zone ($r\omega/c\gg1$, $r/z_0\gg1$):

$$\mathbf{\Pi}^>\sim\hat{\mathbf{z}}pr^{-1}e^{i[(\omega/c)r-\omega t]}\left[\frac{2\frac{\omega}{c}\cos\theta}{\zeta+\epsilon\zeta_0}e^{i\zeta z_0}\right]\ , \tag{17}$$

where

$$\begin{aligned}\zeta&=\frac{\omega}{c}(\epsilon-\sin^2\theta)^{1/2}\ ,\\ \zeta_0&=\frac{\omega}{c}(1-\sin^2\theta)^{1/2}=\frac{\omega}{c}\cos\theta\ ,\end{aligned} \tag{18}$$

and where θ is the angle of observation, defined following Eq. (10). One also finds

$$\mathbf{E}\sim\hat{\theta}p\left[\frac{\omega}{c}\right]^2 r^{-1}e^{i[(\omega/c)r-\omega t]}F_z e^{i\zeta z_0}\ , \tag{19}$$

where

$$F_z=-\frac{2\sin\theta\cos\theta}{(\epsilon-\sin^2\theta)^{1/2}+\epsilon\cos\theta}\ . \tag{20}$$

The power radiated per unit solid angle $dW/d\Omega$ [Eq. (10)] is therefore given by

$$\frac{dW}{d\Omega}=\frac{c}{8\pi}\left[\frac{\omega}{c}\right]^4 p^2\,|F_z|^2 e^{-\mu z_0}\ , \tag{21}$$

where

$$\mu=2\,\mathrm{Im}(\zeta)=2\frac{\omega}{c}\mathrm{Im}(\epsilon-\sin^2\theta)^{1/2}\ . \tag{22}$$

The function $\mu=\mu(\theta)$ should not be confused with the usual absorption coefficient, which it equals when $\theta=0$.

If $\epsilon=1$, then $|F_z|^2=\sin^2(\theta)$ and $\mu=0$, and Eq. (21) becomes identical to the standard result for a dipole in a vacuum. Otherwise, in Eq. (21), the factor $\exp(-\mu z_0)$ arises from absorption, while the ratio of $|F_z|^2$ to $\sin^2(\theta)$ is determined by the other effects of the medium: altered emission at the source, reflection, and refraction.

For normally incident plane waves, it can be shown that the reflection coefficient of the interface is the same for waves approaching from inside the medium as for waves incident from the vacuum. This suggests that reflection at the interface will significantly reduce luminescence from shiny metal surfaces, and also points out the importance of careful preparation of surfaces in connection with the measurement of luminescence from metals.

The simple physical picture implied by the preceding paragraph should not, however, be taken too literally. For one thing, the familiar (plane-wave) reflection coefficient does not apply to spherical waves. For another, it can be shown from the above solution that the power initially radiated by the dipole is affected both by immersion in the medium and by the presence of the interface.

B. Dipole oriented parallel to the surface

The calculation of radiation from a dipole oriented parallel to the surface proceeds along the same lines as outlined above. This time, the coefficient $\mathbf{A}$ of Eq. (11) is directed parallel to the dipole, while $\mathbf{A}$ and $\mathbf{A}'$ each has two components: one parallel to the dipole, and one along z. The boundary conditions, continuity of tangential components of $\mathbf{E}$ and $\mathbf{H}$, are equivalent to four scalar relations [including (15b) but not (15a)]. These four conditions, together with Eqs. (8), suffice to determine the coefficients.

Consider a dipole oriented parallel to the surface and in the plane of observation, i.e., in the x direction [see the definitions following Eq. (10)]. Then $\mathbf{p}=\hat{\mathbf{x}}p$. The resulting field $\mathbf{E}$ in the far zone is

$$\mathbf{E}\sim\hat{\boldsymbol{\theta}}p\left[\frac{\omega}{c}\right]^2 r^{-1}e^{i[(\omega/c)r-\omega t]}F_x e^{i\zeta z_0}\ , \tag{23}$$

where

$$F_x=\left[\cos\theta+\frac{(\epsilon-1)\sin^2\theta}{(\epsilon-\sin^2\theta)^{1/2}+\epsilon\cos\theta}\right]\times\left[\frac{2\cos\theta}{(\epsilon-\sin^2\theta)^{1/2}+\cos\theta}\right]\ . \tag{24}$$

The power radiated per unit solid angle $dW/d\Omega$ is

$$\frac{dW}{d\Omega}=\frac{c}{8\pi}\left[\frac{\omega}{c}\right]^4 p^2\,|F_x|^2 e^{-\mu z_0}\ . \tag{25}$$

Next, let $\mathbf{p}=\hat{\mathbf{y}}p$, i.e., the dipole is parallel to the surface and perpendicular to the plane of observation. The corresponding results are

$$\mathbf{E}\sim\hat{\boldsymbol{\phi}}p\left[\frac{\omega}{c}\right]^2 r^{-1}e^{i[(\omega/c)r-\omega t]}F_y e^{i\zeta z_0}\ , \tag{26}$$

where

$$F_y=\frac{2\cos\theta}{(\epsilon-\sin^2\theta)^{1/2}+\cos\theta} \tag{27}$$

and

$$\frac{dW}{d\Omega}=\frac{c}{8\pi}\left[\frac{\omega}{c}\right]^4 p^2\,|F_y|^2 e^{-\mu z_0}\ . \tag{28}$$

C. Dipole oriented at angles θ_0,ϕ_0

Consider a dipole oriented at polar and azimuthal angles θ_0, ϕ_0, i.e., $\mathbf{p}=(p\sin\theta_0\cos\phi_0,\ p\sin\theta_0\sin\phi_0,\ p\cos\theta_0)$. This dipole being a linear combination of the three dipoles treated above, the electric field is the same combination of fields. It is useful for what follows to resolve the power radiated per unit solid angle into two polarization components. The component with electric field vector in the plane of observation is found to be

$$\frac{dW_p}{d\Omega}=\frac{c}{8\pi}\left[\frac{\omega}{c}\right]^4 p^2\,|(\sin\theta_0)(\cos\phi_0)F_x+(\cos\theta_0)F_z|^2 e^{-\mu z_0}\ , \tag{29a}$$

and the component with electric field vector perpendicular to the plane of observation is

$$\frac{dW_s}{d\Omega}=\frac{c}{8\pi}\left[\frac{\omega}{c}\right]^4 p^2\sin^2\theta_0\sin^2\phi_0\,|F_y|^2 e^{-\mu z_0}\ . \tag{29b}$$

Throughout, the p and s subscripts denote the portion having electric field, respectively, in the plane of observation, and perpendicular to the plane.

D. Distributions of dipoles

Suppose there are N dipoles, each having moment p, in the neighborhood of $(0,0-z_0)$, and suppose their directions are isotropically distributed. Assume that they oscillate with frequency ω, and radiate independently of each other, i.e., incoherently. Then, the power radiated per unit solid angle is the sum of the following polarization components, obtained from (29):

$$\frac{dW_p}{d\Omega}=\frac{c}{24\pi}\left[\frac{\omega}{c}\right]^4 Np^2 Y_p e^{-\mu z_0}\ , \tag{30a}$$

$$\frac{dW_s}{d\Omega}=\frac{c}{24\pi}\left[\frac{\omega}{c}\right]^4 Np^2 Y_s e^{-\mu z_0}\ , \tag{30b}$$

where functions $Y_p(\omega,\theta)$ and $Y_s(\omega,\theta)$ are given by

$$Y_p = |F_x|^2 + |F_z|^2 , \tag{31a}$$

$$Y_s = |F_y|^2 . \tag{31b}$$

It is also useful to define a function $Y(\omega,\theta)$ by

$$Y = \tfrac{1}{2}(Y_p + Y_s) . \tag{31c}$$

Note that functions Y_p, Y_s, and Y are each identically unity when $\epsilon=1$. $Y(\omega,\theta)$ is interpreted to be the relative yield, i.e., power radiated per unit solid angle, relative to the corresponding quantity in the absence of a medium, for small $z_0[\exp(-\mu z_0)\approx 1]$. In the same way, functions Y_p and Y_s are relative yields for polarization components.

The degree of polarization P may be written as the absolute value of the ratio of the difference between (30a) and (30b), to their sum, i.e.,

$$P = \frac{|Y_p - Y_s|}{Y_p + Y_s} , \tag{32}$$

where an isotropic distribution of directions of the dipoles is still assumed. Note that, according to this model, the degree of polarization (for given θ) depends only on the dielectric function, and is independent of the distance z_0 of the dipoles from the surface.

Next, consider a set of dipoles isotropically directed as above, uniformly distributed throughout the medium, and having a distribution of frequencies. Again, assume that they radiate incoherently. Let $f(\omega)$ be the sum of the squares of the dipole moments per unit frequency per unit volume. That is,

$$\sum_i{}' p_i^2 = f(\omega)\Delta\omega\Delta V ,$$

where the sum extends only over those dipoles having their frequency between ω and $\omega+\Delta\omega$ and lying in a particular volume ΔV, for small $\Delta\omega$, ΔV. Substituting $f(\omega)d\omega dV$ for Np^2 in (30) and integrating over z_0 gives the spectral radiance $R = dW/(d\Omega d\omega dA)$, the power radiated per unit solid angle per unit frequency per unit surface area. The two polarization components are

$$R_p(\omega,\theta) = \frac{c}{24\pi}\left[\frac{\omega}{c}\right]^4 f(\omega) Y_p \frac{1}{\mu} , \tag{33a}$$

$$R_s(\omega,\theta) = \frac{c}{24\pi}\left[\frac{\omega}{c}\right]^4 f(\omega) Y_s \frac{1}{\mu} . \tag{33b}$$

In case ultraviolet light, e.g., is used to stimulate luminescence, one might take the spatial distribution of dipoles created in the solid to be proportional to $\exp(-\alpha z_0)$, where α is a constant describing the attenuation of the incident radiation with depth. Integration of Eq. (30) using this density function yields expressions identical to (33), except that $\mu+\alpha$ appears in place of μ, and $f(\omega)$ is to be evaluated at $z_0=0$.

III. CALCULATIONS AND COMPARISON WITH EXPERIMENT

Analysis of experimental luminescence yields using the results given above is straightforward if ϵ is known, when radiance can be assumed to result from radiative transitions in the medium. In many cases, it should be a good approximation to assume an isotropic distribution of directions of equivalent radiating dipoles generated by charged particle or photon irradiation of a solid. Then one may be able, using the present theory, to distinguish features of the experimental data that contain information about the radiative transitions from features associated with the optical properties of the medium. Thus, sharp peaks or abrupt changes in slope in the frequency dependence of Y or Y/μ (whichever is appropriate) should be expected to occur in the experimental spectrum as well, and should not be considered necessarily to correspond to singularities in the primary emission process. Furthermore, to deduce the unknown $f(\omega)$, i.e., the frequency distribution of the effective squared dipole moment, from the measured spectral radiance at fixed angle, one may in principle divide the experimental spectral radiance by the appropriate one of the above expressions.

A. Aluminum

An example of the effect of the dielectric properties of a free-electron-like material on the fluorescence spectrum may be seen in the case of aluminum. Figure 1(a) shows Y as a function of photon energy, calculated from the optical properties of this metal[15,16] using Eq. (31), for four different values of θ, the angle of observation measured from the surface normal. As pointed out in Sec. II, this quantity Y is the relative spectral radiance (i.e., relative to the value when $\epsilon=1$) for an isotropically oriented distribution of oscillators in the medium lying close to the surface ($\mu z_0 \ll 1$). Also, Y gives the shape of the luminescence spectrum from such a collection of oscillators when their frequencies are distributed such that $\omega^4 f(\omega)$ is constant.

As Fig. 1(a) shows, the maximum value of Y increases with θ for small θ, and then decreases, going to zero at 90°. One also sees that the peak positions increase with θ. The formulas of Sec. II show that Y at fixed θ has its maximum at the frequency where $\epsilon_1 = \sin^2\theta$, when ϵ_2 is identically zero. For angles 0°, 30°, and 60°, these energies are 15.1, 17.3, and 29.1 eV, respectively, in aluminum. The maxima in Fig. 1(a) lie slightly lower in energy than these values, due to the occurrence of nonzero ϵ_2.

As discussed in Sec. II Y/μ is the function that describes the effect of the medium upon the radiation originating from oscillators that are distributed uniformly throughout the medium (as well as being randomly oriented in direction). Values of Y/μ calculated from Eqs. (22) and (31) for aluminum at various angles θ are shown in Fig. 1(b). As comparison with Fig. 1(a) shows, the peaks in Y are replaced by rounded steps in Y/μ, in free-electron-gas metals, such as aluminum. For given θ, and small ϵ_2, the position of the step, i.e., of the

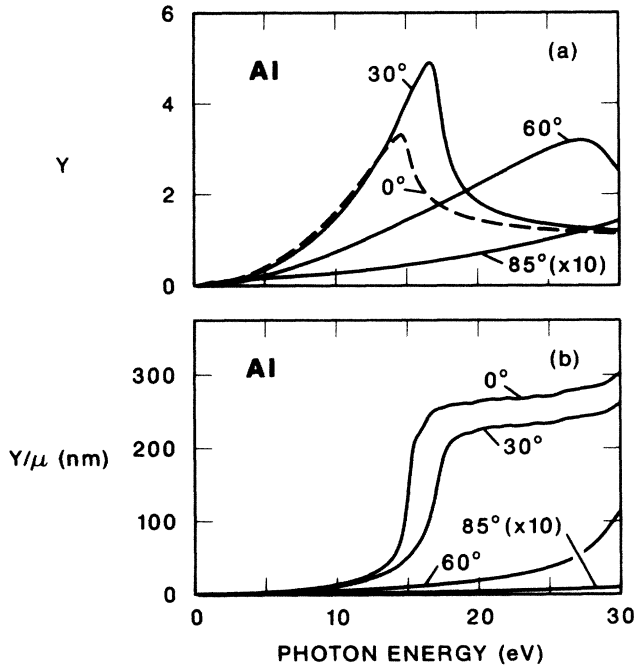

FIG. 1. (a) Y and (b) Y/μ for aluminum metal, at four angles of observation relative to the surface normal, as functions of energy of emitted photons. These functions describe the effect of the optical properties of the medium upon luminescence from randomly directed oscillators located (a) near the surface, or (b) throughout the solid. See Eqs. (31) and (33).

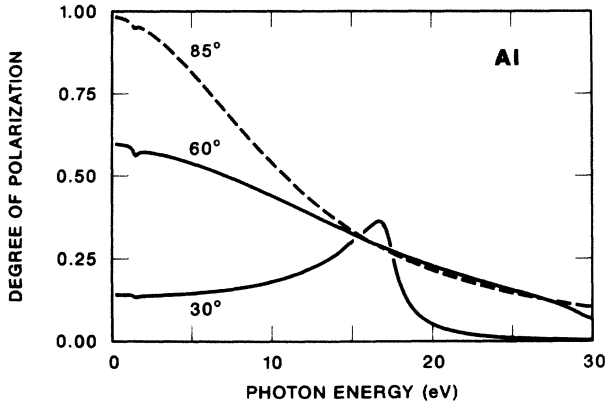

FIG. 2. Degree of polarization of luminescence from aluminum at three angles of observation. A distribution of randomly directed dipoles in the medium is assumed [Eq. (32)]. Except at 0°, the radiation is partially p polarized.

inflection point in the Y/μ curve, is very close to the energy where $\epsilon_1 = \sin^2\theta$.

The degree of polarization P calculated from Eq. (32) for aluminum, for three different angles of observation, is shown in Fig. 2. The degree of polarization at $\theta = 0$ is trivially zero. Otherwise, the p polarization component is larger than the s one. This figure shows that, although P tends to increase with θ, the relationship is not always monotonic.

Luminescence in the visible has been observed from ion-bombarded aluminum and attributed to radiative transitions in the medium.[17] The spectrum consists of a single broad peak around 5200 Å, or 2.4 eV. Remarkably, no significant degree of polarization was found for any angle of observation. Referring to Fig. 2, one expects $P > 0.55$ at 2–3 eV for $\theta \geq 60°$, if the radiation arises from randomly directed oscillators in aluminum metal. Recalculation of P for dipoles having random directions in the xy plane only (i.e., parallel to the surface) improves agreement with experiment by only a negligible amount, since $|F_z|^2/|F_x|^2 \ll 1$ at 2–3 eV, owing to the large magnitude of ϵ. Perhaps the lack of polarization in this experiment is due to surface roughness of the experimental sample, or some other aspect of the surface condition that is not accounted for in the theory.

There are no published observations of vacuum ultraviolet luminescence not attributable to other mechanisms, i.e., to transition radiation, bremsstrahlung, or radiation from roughness-coupled nonradiative surface plasmons.

B. Carbon

Another interesting example is carbon. Figure 3(a) shows structure in Y for glassy carbon that differs qualitatively from that seen for aluminum. Of course, the optical constants[18,19] of these substances differ considerably. We observe that for $\theta \lesssim 30°$, Y has an inverse

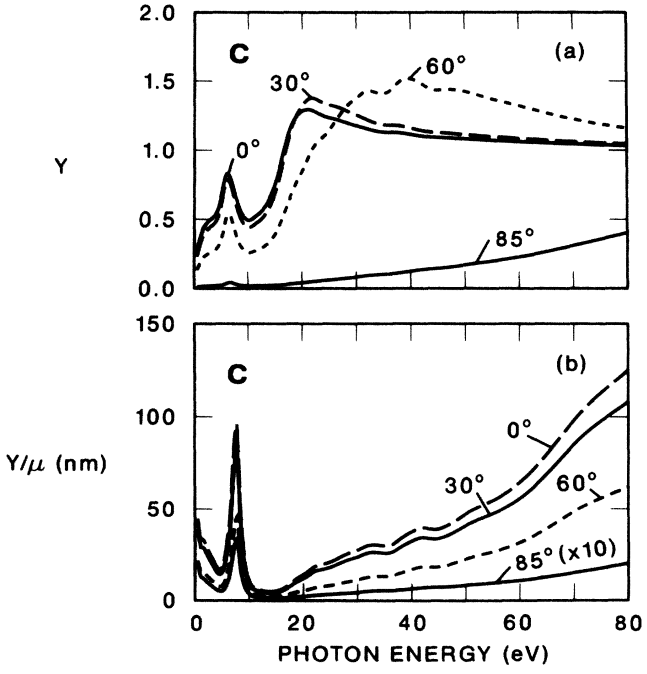

FIG. 3. (a) Y and (b) Y/μ for glassy carbon, at four angles of observation, as functions of energy of emitted photons. This is calculated from Eq. (31).

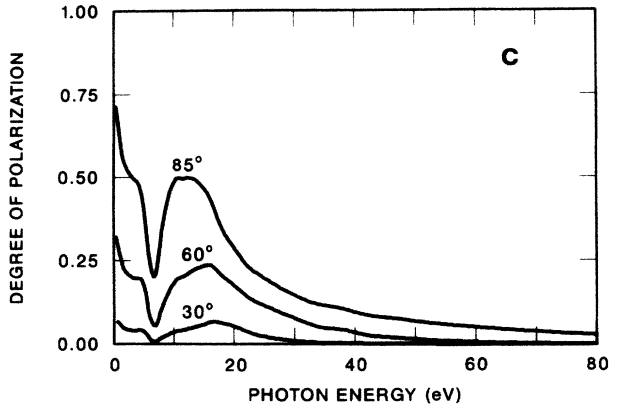

FIG. 4. Degree of polarization of luminescence from glassy carbon at three angles of observation, calculated from Eq. (32). The radiation is partially p polarized.

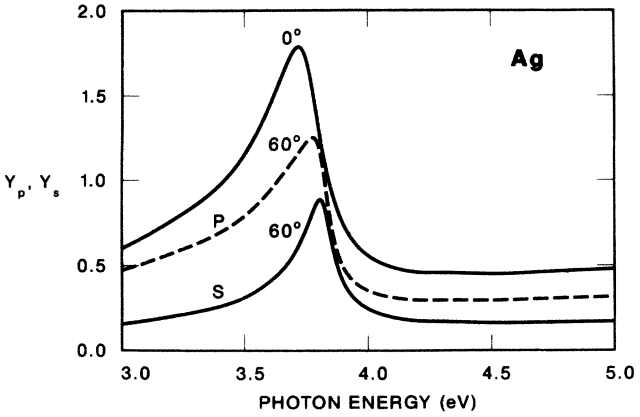

FIG. 5. Y_p and Y_s for two angles of observation in silver vs energy of emitted photons, assuming a uniform distribution of dipole directions. At 0°, Y_p and Y_s are identical in this model.

correlation with n, the real part of the complex refractive index, i.e., the minima and maxima in n correspond to the maxima and minima, respectively, in Y. To explore this relationship further, we rewrite Y in terms of n and k, where $n+ik=(\epsilon_1+i\epsilon_2)^{1/2}$. We find that at $\theta=0$, $Y=4/[(n+1)^2+k^2]$. Since, for carbon, $n \geq k$ everywhere, and $k<1$ for $\hbar\omega>1$ eV, the above expression becomes $Y \approx 4/(n+1)^2$ $(\theta=0)$.

Figure 3(b) shows Y/μ for four angles of observation. Recall that, in aluminum (and free-electron gases), peaks in Y become steps in Y/μ. However, one sees that in glassy carbon, the 6-eV peaks in Y are replaced by 8-eV peaks in Y/μ, while the higher-energy maxima in Y do not have evident counterparts in Y/μ.

Figure 4 shows the degree of polarization P of luminescence from glassy carbon, as calculated from Eq. (32). One sees that P apparently increases monotonically with θ, and that features appear in P that correlate with the low-energy structure in Y.

C. Silver

Metallic silver is a clear case of a medium whose optical properties are crucial to the fluorescence spectrum. Figure 5 shows calculated values of Y_p and Y_s for two values of θ. (At 0°, these two functions are identical.) Sharp maxima appear near the energy $\hbar\omega_p$ of the radiative surface plasmon at $k=0$, 3.76 eV, where $\epsilon=0$.[19] (This is also the energy of the volume plasmon, which, being a longitudinal wave, is not significant here.) The energy of the maximum shifts up only slightly with an increase in angle of observation, and some polarization (see Fig. 6) appears, with the p component being the larger one. Nonradiative surface plasmons (at 3.6 eV, where $\epsilon=-1$), do not affect the predictions of this model, since they require the mediation of surface roughness[6] in order to radiate. Plots of Y/μ, not shown, have similar shapes as Y, with maxima at slightly higher photon energies. For example, the peaks in Y (Y/μ) occur at 3.73 (3.80) and 3.79 (3.82) eV at $\theta=0°$ and 60°, respectively.

Boyd and co-workers[12] have reported calculations and measurements of fluorescence from metallic silver, excited by 4.67-eV light. The intensity, measured at $\theta=45°$, displays a sharp asymmetric peak having its maximum at 3.7 eV. This is about 0.1 eV lower than expected on the basis of their calculation and ours. Finding that a rough sample gives a maximum at the same energy, these authors suggest that the discrepancy arises from radiation of the (nominally) nonradiative surface plasmon, at[20] 3.6 eV via surface roughness.

Boyd *et al.*[12] compare their experimental findings with a band-theory calculation of fluorescence. The effect of the optical properties of the medium upon the emitted light are taken into account by means of two factors: $\exp[-\mu(0)z_0]$ and the Fresnel transmission coefficient for the surface. These factors differ from the corresponding ones, $\exp[-\mu(\theta)z_0]$ and Y, respectively, that appear in the present analysis. However, the plots of their product displayed in Ref. 12 for copper, silver, and gold, have structures that are very similar to those

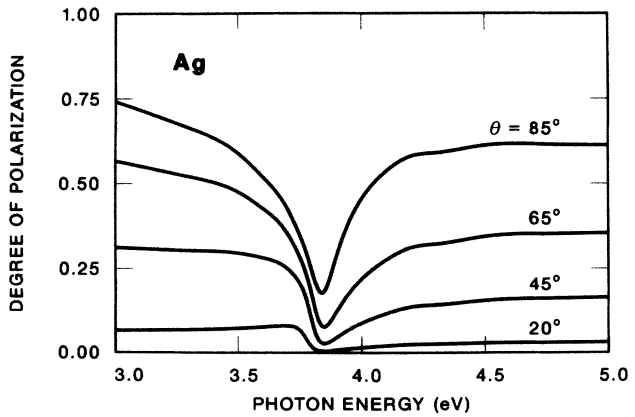

FIG. 6. Degree of polarization of luminescence from silver, at four different angles of observation vs energy $\hbar\omega$ of emitted photons, assuming a uniform distribution of dipole directions. The radiation is partially p polarized.

exhibited by Y and Y/μ as functions of ω.

Luminescence similar to the above fluorescence has been observed in several recent studies employing low-energy electron beams (energy $\lesssim 1$ keV) on massive silver samples. (A reason for considering these low energies is that transition radiation, which for nonrelativistic projectiles is peaked near ω_p, can be neglected.) The photon energy at the intensity maximum at constant θ is 3.78 eV (Ref. 10) (or 3.72 eV) (Ref. 21) for $\theta \lesssim 45°$, and then increases by about 0.05 eV as θ increases to 70°. The emission in this peak is almost unpolarized, for $\theta \lesssim 45°$. The present calculations of Y are in close agreement with these results,[22] giving intensity maxima at 3.73, 3.76, and 3.81 eV for θ values of 0°, 45°, and 70°, respectively, and $P \lesssim 0.1$ for $\theta \lesssim 45°$. The value of the peak intensity is found to be nonzero at 0°, to increase with θ up to about 40°, and then to decrease with further increases in θ. The peak intensities in the calculated Y similarly display a maximum, a broad one at $\theta = 25°$. Other recent measurements,[23] are consistent with the above results.[24]

The electron-induced luminescence at 3.7–3.8 eV discussed above has been attributed to several sources, including decay of volume plasmons,[21] coherent surface bremsstrahlung,[25] and bremsstrahlung.[10,26] Bremsstrahlung is a particularly good candidate mechanism, as it should show a maximum at the observed energy.[26,27] However, the observation of fluorescence[12] discussed above is evidence that excited electronic states within the medium produce luminescence at the same energy. This suggests that the same radiative transitions within the medium might be responsible for luminescence under bombardment by low-energy electrons or other projectiles.

D. Copper

Many authors have reported measurements of luminescence attributed to recombination in copper and gold,[8–10,12,17,25,28–34] accompanying irradiation by low-energy electrons ($\lesssim 1$ keV), ions, and visible and ultraviolet light. These measurements are of particular interest, as they include well-defined spectral features that have been attributed to specific transitions within the metals. We will compare the present theory with the results of Pop *et al.*[33] and Klyap *et al.*[34] involving bombardment by low-energy electrons.

In applying the present theory to these experiments, the smallness of the ranges of low-energy electrons allows one to neglect the effect of absorption, as was done above for silver. This has been carefully checked in the case of 500-eV electrons, which is important in our comparison with experiment. The median ranges R_{50} of 500-eV electrons in copper and gold are 1.4 nm and 0.7 nm, respectively.[35] These ranges are 1–2 orders of magnitude smaller than the relevant values of photon escape depth, $1/\mu$, at the photon frequencies of interest. Under the approximation that the embedded dipoles are all located at $z = -z_0 = -R_{50}$, Eq. (30) may be compared with the experiment. In these cases, however, calculated values of Y are close in value to $Y\exp(-\mu z_0)$, and have negligible difference in shape and positions of structural features, since not only is the factor $\exp(-\mu z_0)$ close to unity but the variation of the factor with ω is similar to the (much larger) variation of Y. Therefore, the exponential factor can be dropped.

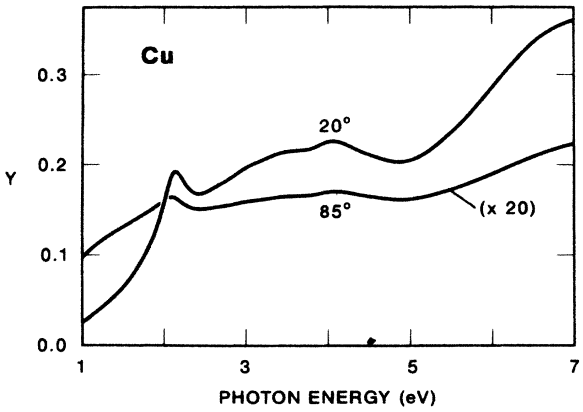

FIG. 7. Y for copper at two angles of observation, as functions of energy of emitted photons.

Figure 7 shows the function Y of metallic copper calculated for two values of θ, 20° and 85°, using optical data from Hagemann *et al.*[19] The values of photon energy at the maxima at 20° (85°) are 2.14 (2.10) and 4.06 (4.14) eV. The spectrum given by Pop *et al.*[33] is remarkably similar. The most pronounced peaks in the experiment are located at 2.15 and 4.0 eV, the latter one being the more intense. The 2.15-eV peak looks similar to the corresponding peak in Fig. 7, but the 4.0-eV peak is sharper. The relative intensity is larger around 4 eV than in the figure, and falls off more rapidly at both ends of the spectrum (below 2 eV and above 4 eV). The experimental peak positions are almost independent of the electron incidence angle and observation angle, except that the main peak varies in the range 3.95–4.20 eV when θ goes from 25° to 85°. The relative intensity at

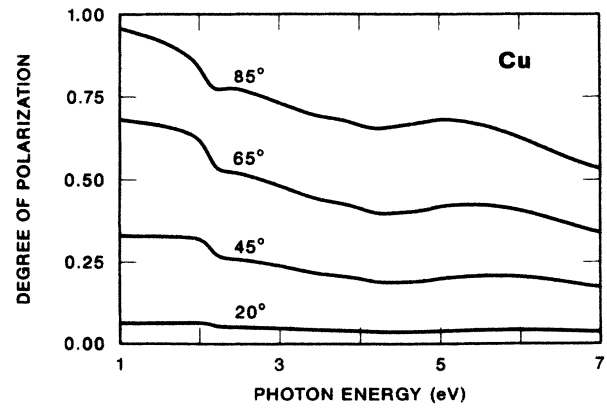

FIG. 8. Degree of polarization of luminescence from copper, at four different angles of observation vs energy of emitted photons, assuming a uniform distribution of dipole directions. The radiation is partially p polarized.

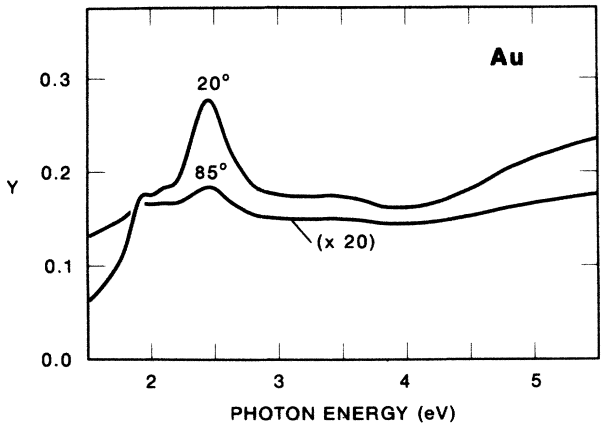

FIG. 9. Y for gold at two angles of observation, as functions of energy of emitted photons.

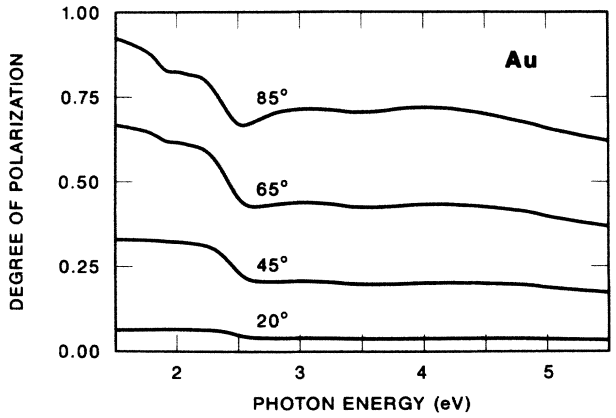

FIG. 10. Degree of polarization of luminescence from gold at four different angles of observation vs energy of emitted photons, assuming a uniform distribution of dipole directions. The radiation is partially p polarized.

the low-frequency end of the measured spectrum (which extends down to 1.8 eV) decreases somewhat with increasing θ, which is not seen in the theory. Both in copper and in gold, the yield, photons per unit solid angle per unit frequency per incident electron (measured at $\hbar\omega = 3.44$ eV), is proportional to electron energy up to about 500 eV,[25] which is consistent with the radiative transitions of excited electrons of the medium.

Figure 8 shows the degree of polarization calculated from Eq. (32) for copper, for four different angles of observation. P is zero at $\theta = 0$ and increases with θ and with wavelength, in agreement with the trends reported for the experiment.[33]

E. Gold

Figures 9 and 10 show the yield function Y and the degree of polarization as calculated for gold. Optical constants measured by Theye[36] and tabulated by Lynch and Hunter[37] were used. The strongest peak occurs at 2.45 eV, in close agreement with the experimental main peak[33] at 2.42 eV. There is, however, a significant difference, in that a degree of polarization amounting to about 33% is measured with $\theta = 20°$, in the neighborhood of the main peak, compared to a value in Fig. 10 of about 6%. At higher frequencies, however, the experimental P does become quite small, in agreement with Fig. 10. That the positions of the main experimental and calculated s and p polarization peaks are essentially the same suggests that their origin lies within the medium, and that the effective dipoles do not necessarily have a peak in their spectrum at 2.42 eV. The excess amount of p polarization then corresponds to an excess of dipoles (in the low-frequency range) directed in the plane of observation, compared with a uniform distribution. It may be significant in this connection that the data discussed here were taken with oblique incidence (75° from the surface normal) of the electron beam.

IV. DISCUSSION AND CONCLUSIONS

We have presented solutions of Maxwell's equations for oscillating dipoles embedded in a dielectric half space. Expressions are given for power radiated per unit solid angle and for degree of polarization for various assumed distributions of dipoles, assumed to radiate incoherently. Results are presented for aluminum, carbon, silver, copper and gold. Detailed comparisons are made with measured fluorescence of silver, and luminescence of silver, copper, and gold under bombardment by low-energy electrons. Positions of the major peaks in the experimental luminescence spectra are found to be reproduced precisely by the present model, starting with an ensemble of oscillators that does not contain any such features in its frequency spectrum. This means that these features in the luminescence spectrum are characteristic of the optical properties of the media, and may not correspond to structures in the density of states of electrons or holes excited by the primary radiation.

ACKNOWLEDGMENTS

This research was sponsored jointly by the Strategic Defense Initiative Organization under DNA Task Code X99QMXXD and Work Unit Code 00003, Air Force Weapons Laboratory, under Interagency Agreement DOE No. 1418-1418-A1 and the Office of Health and Environmental Research, U.S. Department of Energy, under Contract No. DE-AC05-840R21400 with Martin Marietta Energy Systems, Inc.

[1]A. Sommerfeld, Ann. Phys. (N.Y.) **28**, 665 (1909); **81**, 1135 (1926).

[2]See J. Zenneck, Ann. Phys. (N.Y.) **23**, 846 (1907); **28**, 665 (1909); and the discussion in Ref. 3.

[3]J. A. Stratton, *Electromagnetic Theory* (McGraw-Hill, New York, 1941).

[4]See, e.g., *Surface Polaritons,* edited by V. M. Agranovich and D. L. Mills (North-Holland, Amsterdam, 1982).

[5]See, e.g., R. H. Ritchie and H. B. Eldridge, Phys. Rev. **126**, 1935 (1962).

[6]H. Raether, *Excitation of Plasmons and Interband Transitions by Electrons* (Springer-Verlag, Berlin, 1980), Chap. 10.

[7]See, e.g., M. Moskovits, Rev. Mod. Phys. **57**, 783 (1985).

[8]A. Mooradian, Phys. Rev. Lett. **22**, 185 (1969).

[9]O. M. Artamonov and S. N. Samarin, Radiat. Eff. **40**, 201 (1979).

[10]S. S. Pop and V. A. Kritskii, Radiotekh. Elektron. **26**, 2398 (1981) [Radio Eng. Electron. Phys. (USSR) **26**, 107 (1981)].

[11]O. H. Crawford, Oak Ridge National Laboratory Report No. CONF-850484, 1986 (unpublished).

[12]G. T. Boyd, Z. H. Yu, and Y. R. Shen, Phys. Rev. B **33**, 7923 (1986).

[13]J. D. Jackson, *Classical Electrodynamics*, 2nd Ed. (Wiley, New York, 1975).

[14]See Ref. 13, p. 242. The physical value of the time-averaged Poynting vector is the real part of the expression for it written here; such convention is also followed for the fields.

[15]E. Shiles, T. Sasaki, M. Inokuti, and D. Y.Smith, Phys. Rev. B **22**, 1612 (1980).

[16]J. H. Weaver, C. Krafka, D. W. Lynch, and E. E. Koch, *Optical Properties of Metals*, Vol. 18-2 of *Physik Daten* (Fachinformationszentrum, Karlsruhe, 1981).

[17]M. Zivitz and E. W. Thomas, Phys. Rev. **13**, 2747 (1976).

[18]M. W. Williams and E. T. Arakawa, J. Appl. Phys. **43**, 3460 (1972).

[19]H.-J. Hagemann, W. Gudat, and C. Kunz, J. Opt. Soc. Am. **65**, 742 (1975); DESY Report No. SR-74/7, 1974 (unpublished).

[20]P. Zacharias, Z. Phys. **238**, 172 (1970).

[21]S. S. Pop, V. A. Kritskii, and I. P. Zapesochnyi, Pis'ma Zh. Tekh. Fiz. **5**, 1542 (1979) [Sov. Tech. Phys. Lett. **5**, (12), 613 (1979)].

[22]It is a good approximation to neglect the absorption factor, $\exp(-\mu z_0)$, as $\mu z_0 \ll 1$, for low-energy (<1 keV) electrons in silver, especially since, as mentioned above, Y and Y/μ have similar structures at nearly the same values of ω.

[23]V. A. Kritskii, S. S. Pop, and I. P. Zapesochnyi, Izv. Akad. Nauk. SSSR Ser. Fiz. **43**, 478 (1979) [Bull. Acad. Sci. USSR Phys. Ser. **43** (3), 25 (1979)].

[24]Besides the luminescence at 3.7–3.8 eV discussed above, a p-polarized emission peaking at 3.5 or 3.6 eV begins to appear as θ is taken above approximately 45° (see Refs. 10 and 21). This is presumably due to roughness-coupled radiation from nonradiative surface plasmons, which appear to make a similar contribution to fluorescence also (Ref. 12).

[25]M. P. Klyap, V. A. Kritskii, and S. S. Pop, Opt. Spectrosk **57**, 944 (1984) [Opt. Spectrosc. (USSR) **57**, 576 (1984)].

[26]H. Boersch, P. Dobberstein, D. Fritzsche, and G. Sauerbrey, Z. Phys. **187**, 97 (1965); H. Boersch and G. Sauerbrey in *Optical Properties and Electronic Sturcture of Metals and Alloys*, edited by F. Abeles (North-Holland, Amsterdam, 1966), p. 386.

[27]There is a close connection between bremsstrahlung from low-energy (nonrelativistic) electrons, and the emissions studied in this work. In lowest order in $\beta = v/c$, bremsstrahlung may be represented as arising from a distribution of oscillating dipoles within the medium, fixed in place and having a very broad frequency distribution. The theory for the intensity of the p- and s-polarization components should therefore reduce to expressions of the form of Eq. (29) integrated over the joint distribution of z_0 and dipole directions. See R. H. Ritchie, J. C. Ashley, and L. C. Emerson, Phys. Rev. **135**, 1759 (1964).

[28]A. Bonnot, J. M. Debever, and J. Hanus, Solid State Commun. **10**, 173 (1972).

[29]C. Kerkdijk and E. W. Thomas, Physica (Utrecht) **63**, 577 (1973).

[30]B. G. Papanicolaou, J. M. Chen, and C. A. Papageorgopoulos, J. Phys. Chem. Solids **37**, 403 (1976).

[31]P. Borziak, I. Konovalov, Yu. Kulyupin, and K. Pilipchak, Thin Solid Films **35**, L9 (1976).

[32]V. A. Kritskii, S. S. Pop, and V. G. Drobnich, Izv. Akad. Nauk SSSR, Ser. Fiz. 2600 (1976) [Bull. Acad. Sci. USSR, Phys. Ser. **40** (12), 132 (1976)].

[33]S. S. Pop, V. A. Kritskii, M. P. Klyap, and I. P. Zapesochnyi, Fiz. Tverd. Tela (Leningrad) **23**, 2052 (1981) [Sov. Phys.—Solid State **23**, 1197 (1981)].

[34]M. P. Klyap, V. A. Kritskii, Yu. A. Kulyupin, Yu. N. Kucherenko, K. N. Pilipchak, and S. S. Pop, Zh. Eksp. Teor. Fiz. **86**, 1117 (1984) [Sov. Phys.—JETP **59**, 653 (1984)].

[35]H. Iskef, J. W. Cunningham, and D. E. Watt, Phys. Med. Biol. **28**, 535 (1983).

[36]M. L. Theye, Phys. Rev. B **2**, 3060 (1970).

[37]D. W. Lynch and W. R. Hunter, in *Handbook of Optical Constants of Solids*, edited by E. D. Palik (Academic, Orlando, 1985), pp. 286–289.